

Using photoactivated periodate to decompose TOC from hydrolysates of chemical warfare agents

Xueming Tang^a, Linda K. Weavers^{b,*}

^a Environmental Science Graduate Program, The Ohio State University, Columbus, OH 43210, USA

^b Department of Civil and Environmental Engineering and Geodetic Science,
The Ohio State University, Columbus, OH 43210, USA

Received 22 March 2007; received in revised form 18 June 2007; accepted 13 August 2007

Available online 19 August 2007

Abstract

Photoactivated periodate was investigated for the disposal of hydrolysates of chemical warfare agents (HCWAs) when hydrolysis is used as the first step in disposal of chemical warfare agents (CWAs). The kinetics and mechanisms of total organic carbon (TOC) loss by photoactivated periodate oxidation of the HCWAs, thiodiglycol (TDG), 3,3-dithiopropanol (TDP), and 1,4-thioxane (TX), were investigated at pH 3, 7, and 10. At pH 3, TDG had the fastest rate of TOC loss followed by TDP and TX. Less TOC loss at pH 7 compared to pH 3 was attributed to ozone decomposition reactions and OH• quenching by mineralization products (e.g., bicarbonate) at pH 7. At pH 10, compared to pH 7, TX had more TOC loss, but TDG and TDP exhibited similar TOC loss as pH 7 conditions. In all experiments, TOC loss ceased when periodate was depleted. Solution conditions such as pH, initial ratio of periodate to HCWA, nitrogen purging, and consecutive additions of periodate were investigated to explore the role of reactive species in TOC loss and to determine optimal periodate mineralization conditions for HCWAs. In all cases consecutive additions of periodate provided the most TOC loss but the conditions for the most efficient use of periodate was different for each HCWA.

© 2007 Elsevier B.V. All rights reserved.

Keywords: Thiodiglycol; 3,3-Dithiopropanol; 1,4-Thioxane; TOC; Hydroxyl radical; Iodyl radical; Ozone

1. Introduction

The United States and Russia have had stockpiles of chemical warfare agents (CWAs) for more than 50 years [1,2]. The stockpile of CWAs in the United States consists of two classes of extremely hazardous agents: nerve agents, such as GB (Sarin) and VX (methylphosphonothioic acid); and blister or mustard agents, such as H (70% mustard), HD (pure mustard), and HT (60% mustard) [1]. Because these agents have been stored for decades, they are deteriorating and have increased risks of leaking. A range of disposal technologies have been evaluated since the 1970s. Currently, neutralization by hydrolysis is an accepted approach to decompose HD and VX [3]. However, hydrolysates of HD and VX are not completely harmless components; further treatment of the hydrolysates is required prior to final disposal.

Furthermore, biodegradation is accepted but requires storage and transport of hydrolysates during which time hydrolysates may undergo side reactions to form harmful or more toxic products [3].

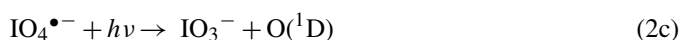
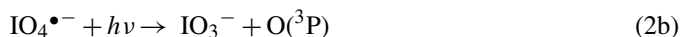
Advanced oxidation processes (AOPs) are technologies capable of degrading persistent chemicals and recalcitrant pollutants in the environment [4–6]. Highly reactive and nonselective species, mainly hydroxyl radicals (OH•) are generated *in situ* to oxidize compounds under ambient conditions. Mineralization can be achieved under certain conditions [4,6]. One novel AOP, photoactivated periodate, is being explored [7–11]. It has rapidly decomposed 2-chlorobiphenyl and chemical oxygen demand (COD) associated with triethanolamines [7,8]. In another study the degradation rate of 4-chlorophenol experienced only a minor decline in the presence of the OH• scavenger, *t*-butanol, demonstrating the importance of reactive species other than OH• [10]. Under UV irradiation, photoactivated periodate generates a number of reactive species including: OH•, periodyl radical (IO₄• or I^{VIII}), iodyl radical (IO₃• or I^{VI}), hydrogen

* Corresponding author. Tel.: +1 614 292 4061; fax: +1 614 292 3780.
E-mail address: weavers.1@osu.edu (L.K. Weavers).

peroxide (H_2O_2), atomic oxygen, and ozone (O_3) [12–15]. These reactants react with compounds and may eventually mineralize reduced compounds in the mixture.

Periodic acid exists as an equilibrium mixture of a variety of species depending on pH, concentration, and the presence of other components in aqueous solutions. The monoanionic dehydrate, IO_4^- , is the predominant species in acidic solution. In dilute alkaline solution, the monomeric periodate ions are $\text{H}_3\text{IO}_6^{2-}$ and $\text{H}_2\text{IO}_6^{3-}$ [16–18]. In concentrated alkaline solution, the dimmer, paraperiodate, $\text{H}_2\text{I}_2\text{O}_{10}^{4-}$, is formed from $\text{H}_3\text{IO}_6^{2-}$ [16].

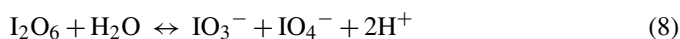
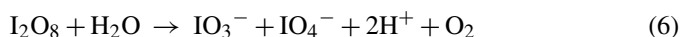
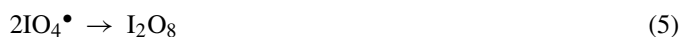
A reaction scheme for photolysis of periodate between pH 2.44 and 4.90 was proposed by Wagner and Strehlow [14]. Upon UV irradiation, IO_4^- is excited and generates primary radicals $\text{O}^{\bullet-}$, IO_3^{\bullet} , $\text{O}(^3\text{P})$ (triplet state atomic oxygen), and $\text{O}(^1\text{D})$ (singlet state atomic oxygen):



These primary radicals further react with H^+ , O_2 , IO_4^- and form intermediate reactive species, including, IO_4^{\bullet} , H_2O_2 and O_3 :



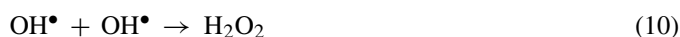
IO_4^- can be regenerated through dimerization of IO_4^{\bullet} and IO_3^{\bullet} :



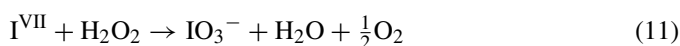
However, high concentrations of IO_4^- are suspected to quench OH^{\bullet} as shown in Eq. (3) [19]. Therefore, optimizing the ratio of periodate to organic reactant may be an important parameter in the reaction systems. In the presence of oxygen, $\text{O}(^3\text{P})$ is quenched by O_2 to form O_3 (Eq. (4)). In oxygen limited environments, O_2 is produced either by recombination of $\text{O}(^3\text{P})$ (Eq. (9)) or by decomposition of dimer species of IO_4^{\bullet} (Eq. (6)):



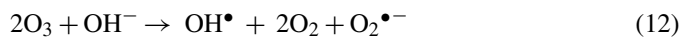
H_2O_2 is produced either by recombination of OH^{\bullet} (Eq. (10)) or by hydrolysis of O_3 [22]:



In acidic solutions, both O_3 and H_2O_2 react slowly with IO_4^- [12,20]. Whereas in alkaline solutions, H_2O_2 reacts rapidly with periodate (I^{VII}) to form iodate (IO_3^-) [12,21]:



In alkaline solution, ozone is decomposed by hydroxide forming hydroxyl radical [22]:



Previous work in this laboratory established that IO_3^{\bullet} and $\text{O}(^3\text{P})$ were important species for degradation of 4-chlorophenol in the photoactivated periodate system with a monochromatic light source at pH 3 [10]. At pH 10, both I^{VI} and OH^{\bullet} played important roles in degradation of hydroxylalkyl sulfides in the photoactivated periodate system under a 220 nm monochromatic light irradiation [11]. In our current work, different organic substrates, namely three HCWAs, the main hydrolysate product of HD, thiodiglycol (TDG, $\text{HO}(\text{CH}_2)_2\text{S}(\text{CH}_2)_2\text{OH}$), and minor hydrolysates of HD, 3,3-dithiopropanol (TDP, $\text{HO}(\text{CH}_2)_3\text{S}(\text{CH}_2)_3\text{OH}$), and 1,4-thioxane (TX, $\text{S}(\text{CH}_2)_2\text{O}$), were investigated with a polychromatic light source under different pH conditions. By monitoring IO_4^- , IO_3^- , O_3 , and TOC, direct evidence of photoactivated periodate reaction pathways were observed. The goal of this research was to elucidate photoactivated periodate as a potential technology to decompose TOC from hydrolysis products of chemical warfare agents (HCWAs) and optimize the pH and the ratio of periodate to HCWAs in the reaction.

2. Methodology

2.1. Materials

All reagents used in this study were of reagent grade or higher except where specified. Periodic acid, sodium iodate, perchloric acid, lithium hydroxide, sodium boro-hydrate, 37% formaldehyde stabilized solution, horseradish peroxidase, and *p*-hydroxylphenyl acetic acid were obtained from Fisher Scientific. Thiodiglycol (2,2-thiodiethanol), 3,3-thiodipropanol, 1,4-thioxane, and purpald (4-amino-5-hydrazino-1,2,4-triazole-3-thiol) were from Sigma-Aldrich. Potassium ferrioxalate was purchased from Alfa Aesar. NMR analysis of thiodiglycol sulfoxide (TDGO, Chem Service Inc.) suggested that the two compounds in the TDGO standard were the inter-conversion isomers of TDGO. Deionized water from a Milli-Q system (Milli-RX45, Milli-pore) was used for all experiments.

2.2. Experimental setup

2.2.1. Reactor

In order to prevent any potential reactions with laboratory fluorescent light, all experiments were carried out inside of a black-painted wooden box (0.8 m × 1.2 m × 1.1 m). The photochemical reactor utilized in this study contained six vertical ports on the top of a 500 mL water-jacketed glass cylindrical reactor with a quartz irradiated surface. In N_2 purging experiments, these ports served as a sampling location, N_2 gas purging inlet/outlet, dissolved oxygen probe (Orion 810) inlet, Sure-flow Ross semi-micro pH electrode (ThermoOrion) inlet, and autotitrator of a pH-stat controller (PHM 290, Radiometer/Copenhagen) inlet.

For experiments exclusive of N₂ purging, the two purging ports were used as a Tedlar gas bag inlet to keep isobaric reaction conditions and a sealed port. The temperature of solution within the reactor was maintained at 21 ± 1 °C by a water bath (ISOTEMP 1006S, Fisher Scientific). The distance from the light output to the irradiated surface of the reactor was approximately 49 mm. Dark reactions were conducted in the same reactor but in the absence of light.

2.2.2. Light source

The light source of the photochemical experiments in this study was a 500 W Hg(Xe) arc lamp (Oriol 66142) installed in a lamp housing with a built in ignitor (Oriol 66028) and an arc lamp power supply (Oriol 68811). Prior to all light experiments the Hg(Xe) lamp was stabilized for no less than 1 h. Intense polychromatic irradiation was filtered by a water filter prior to the reaction to reduce IR irradiation. The intensity of the light was measured by the Hatchard-Parker/Ferrioxalate actinometer [23,24].

2.2.3. Solution preparation and reaction conditions

0.25 M periodic acid, 0.25 M TDG, 0.1 M TDP, and 0.1 M TX stock solutions were stored at 4 °C covered with aluminum foil to avoid light reactions. Before experiments, 500 mL of the appropriate concentration of periodic acid was prepared from the stock solution. In order to prevent sodium periodate precipitation at high pH, LiOH instead of NaOH was used to adjust the pH. The initial pH of the reaction solution was adjusted by fresh filtered 5N LiOH. One normality of LiOH or 1.5 HClO₄ was used in a pH-stat system (PHM 290, Radiometer) to maintain the desired pH. All experiments were stirred using a magnetic stir bar. Control experiments indicated this provided adequate stirring. For N₂ purging experiments (99.999% purity N₂ gas), 600 mL min⁻¹ of N₂ was purged through a small glass gas dispersion tube with coarse porosity outlet. No significant TOC loss was measured in control experiments during N₂ purging.

2.2.4. Sampling

Before each experiment, 10 mL of sample was analyzed to determine the initial concentration of periodate and to verify the absence of iodate, H₂O₂, formaldehyde, and O₃. Next, an appropriate quantity of HCWA stock solution was introduced into the photochemical reactor to have a reaction volume ranging from 492.5 to 495.0 mL.

At selected time intervals, 6–8 mL samples were collected in amber glass vials. Except for O₃ measurements, samples were purged with nitrogen gas (99.999% purity) for 5 min to remove residual ozone. For HCWAO analysis, 2 mL samples were added to 4 mL of 0.05 M barium hydroxide solution to quench residual periodate. A 0.45 µm PVDF filter (Whatman, 6872-1304) connected to a pre-wetted IC-H cartridge (Alltech 30264) was applied to remove insoluble barium salts and exchange extra barium cations with protons to avoid the formation of barium carbonate precipitates from contact with ambient air. Due to large sample volume requirements each experimental condition was run twice sampling at different time points in order to keep

changes in the volume of the reaction system to within 15% during the course of reactions. Selected experimental conditions were conducted multiple times to ensure reproducibility. Error (1S.D.) is reported only for experiments in which multiple runs were conducted.

2.2.5. Analytical procedures

Analysis of periodate and iodate, was conducted by a HP^{3D} Capillary Electrophoresis system (Agilent) at the wavelength of the highest extinction coefficient of the compound of interest. A standard bare fused silica capillary (40 cm long × 50 µm i.d., G1600-60132) was used to separate ions under 50 mbar injection pressure and –25 kV applied voltage [10,25]. A 100 mM acetate buffer at pH 4.45 was used as a carrier buffer and buffer was replenished after each sample measurement. The capillary was preconditioned by flushing the capillary with 100 mM acetate buffer for 5 min before each run and was cleaned by a Milli-Q water sample after every three samples. Analysis lasted 8 min and the retention times were 3.2 and 4.8 min for periodate and iodate, respectively.

Organic degradation products, including thiodiglycol sulfoxides (TDGO), were detected by electron spray ionization mass spectrometry (ESI-MS) (Esquire-LC, Bruker) under 50 V of the cone voltage. Peaks of interest were verified by ESI-MS–MS under the positive ionization mode [26]. Samples were composed of a mixture of 50:50 water and methanol at a flow rate of 0.2 mL min⁻¹. Rapid degradation of TDG allowed for TDG to be used as an internal standard for TDGO [11].

Purpald (4-amino-5-hydrazine-3-mercapto-1,2,4-triazole) (AHMT) was applied to determine formaldehyde [11] by a spectrophotometric procedure [27,28]. Briefly, 0.1 mL formaldehyde samples were collected, diluted to 1 mL, derivatized with 1.5 mL 1% AHMT, and incubated at 200 rpm for 30 min. 2.5 mL 0.2% NaBH₄ in 1N NaOH was then added to the solution followed by UV–vis spectrometry (UV-2401 PC, Shimadzu) at 550 nm. Both AHMT and NaBH₄ solutions were prepared directly before each experiment.

Organic ions containing sulfur and anionic degradation products, including sulfate, were identified by negative mode ionization ESI-MS. Aqueous O₃ was determined using the indigo method [29]. Dissolved oxygen (DO) was measured by a DO meter (Oriol 810).

Total organic carbon (TOC) was observed by a TOC analyzer (Shimadzu TOC-5000A) under the non-purgeable organic carbon (NPOC) mode. A mixture of 2 mL sample with 4 mL of HCl acidified Milli-Q water solution was introduced into the TOC analyzer. Calibration samples were run before each experiment. Control experiments with and without sparging of HCHO in concentrations observed in this study indicated that HCHO was not stripped from samples during analysis.

H₂O₂ was identified using fluorescence resonance (RF-5301 PC, Shimadzu). Horseradish peroxidase catalyzes the reaction between hydrogen peroxide and *p*-hydroxylphenyl acetic acid to form a dimer at a one to one ratio and the produced dimer was detected by spectrofluorescence excitation at 326 nm and emission at 405 nm [30,31]. The concentration of the dimer is directly correlated to the hydrogen peroxide concentration.

3. Results and discussion

In order to determine if TOC loss associated with HCWA was due to direct photolysis, photolysis control experiments in the absence of periodate were investigated and showed TOC associated with TDGO decreased by 24% and with TDG decreased by 18% in 5 h [32]. However, all the ϵ_{HCWA} 's are substantially lower than the extinction coefficient of I^{VII} , $\epsilon_{\text{I}^{\text{VII}}}$, resulting in less than 0.01% loss by direct photolysis based on light screening factors [32,33]. The pK_{a} values for all of the HCWAs are higher than 13 indicating that there is no effect of pH on HCWA speciation under our experimental conditions.

Dark reaction kinetics and mechanisms of TDG, TDP, and TX degradation were investigated at pH 3, 7, and 10 as described in Tang and Weavers [11]. The dark reactions at pH 3 and 7 proceeded by oxygen addition to the sulfur atom in HCWAs following second-order kinetics. At pH 10, the dominant periodate species in water changed from IO_4^- to $\text{H}_3\text{IO}_6^{2-}$ and $\text{H}_2\text{I}_2\text{O}_{10}^{4-}$ resulting in both Malaprade and sulfur atom addition reaction pathways [11,18]. No TOC reduction was observed under dark reaction conditions.

3.1. HCWA degradation and by-product formation

Initially, experiments with 30 mM IO_4^- , and 1 mM HCWA were photolyzed at pH 3. Reaction products of TDG are shown in Fig. 1. TDGO was formed and decomposed rapidly and the

formation of formaldehyde was observed. For all HCWAs, significant TOC loss was observed and a mineralization product, SO_4^{2-} , was detected. TOC decreased slowly at the beginning of the reaction but accelerated as the reaction proceeded. As TOC decreased, the concentration of formaldehyde reached a maximum concentration and began to decrease. Periodate was consumed upon photolysis. A mass balance of iodine species shows that iodate is the only photolysis product forming from periodate. Both degradation of TOC and the formation of SO_4^{2-} ceased when periodate was depleted. O_3 and H_2O_2 were formed under photolysis and concentrations decreased as periodate was depleted. At the end of reactions under all conditions reported, iodate, sulfate, and carbon dioxide (assumed based on TOC loss) were the dominant species in solution.

As observed in Fig. 1b, IO_4^- depletion and IO_3^- formation occurred linearly with time under all conditions studied. This trend is consistent with zero-order reaction kinetics of IO_4^- . Zero-order rate constants for periodate are shown in Table 1. The zero-order reaction rate constants of IO_4^- with HCWAs are somewhat higher than without HCWAs. This result suggests that the loss of IO_4^- is not dependent on IO_4^- concentrations but dependent primarily on the light intensity and somewhat on the reactivity of the particular HCWA in the system.

TDP and TX showed similar degradation products to TDG although the maximum concentrations and degradation times were shifted (data not shown). Based on second-order reaction rate constants, HCWAs were oxidized to HCWA sulfoxides (HCWAOs) completely in 1.3 min for TDG, in 0.8 min for TX, and in 0.3 min for TDP [32]. H_2O_2 production was comparable for all HCWAs, whereas the maximum O_3 measured in solution was much higher in the TX (0.27 mM) system than with TDG (0.19 mM) and TDP (0.14 mM). When using the same initial concentration of periodate, the total amount of reactive species generated from primary periodate photolysis reactions (generation only, not considering loss) is expected to be the same with any of the HCWAs. The higher concentration of O_3 suggests that consumption by either $\text{O}(^3\text{P})$, O_3 , or both is less in the TX system compared to TDG and TDP. We expect that the steric structure of TX or the oxidation products of TX are less reactive with $\text{O}(^3\text{P})$ or O_3 than the linear structure of TDG and TDP.

3.2. Effect of periodate concentration

Next, the effect of periodate concentration on HCWA degradation was investigated as shown in Fig. 2. TOC loss occurred

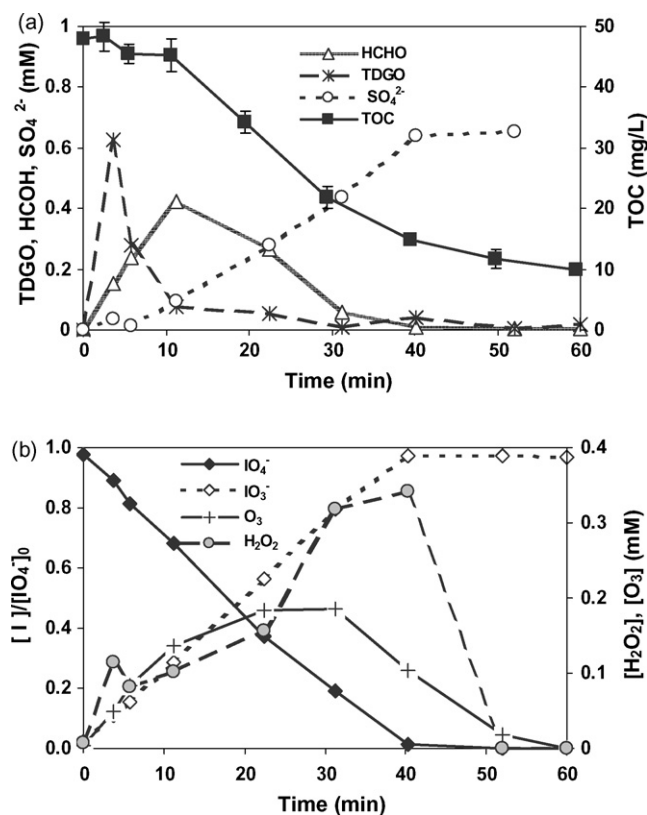


Fig. 1. Photolysis of 30 mM IO_4^- with 1 mM TDG at pH 3. $[\text{I}]$ represents the iodine species of interest and $[\text{IO}_4^-]_0$ is the periodate concentration in the system initially.

Table 1
Zero-order periodate reaction rate constants during photolysis with and without the presence of HCWAs (1 mM) under various conditions

HCWA	$k_{\text{IO}_4^-}$ ($\times 10^{-6} \text{ M}^{-1} \text{ s}^{-1}$)			
	pH 3	pH 7	pH 10	pH 3 purging
No HCWA	10.2	5.5	1.2	ND ^a
TDG	12.8 \pm 0.4	8.6	1.6	12.1
TDP	12.2 \pm 0.4	7.4	2.3	12.6
TX	11.1 \pm 0.7	8.8	2.9	11.4

^a Not determined.

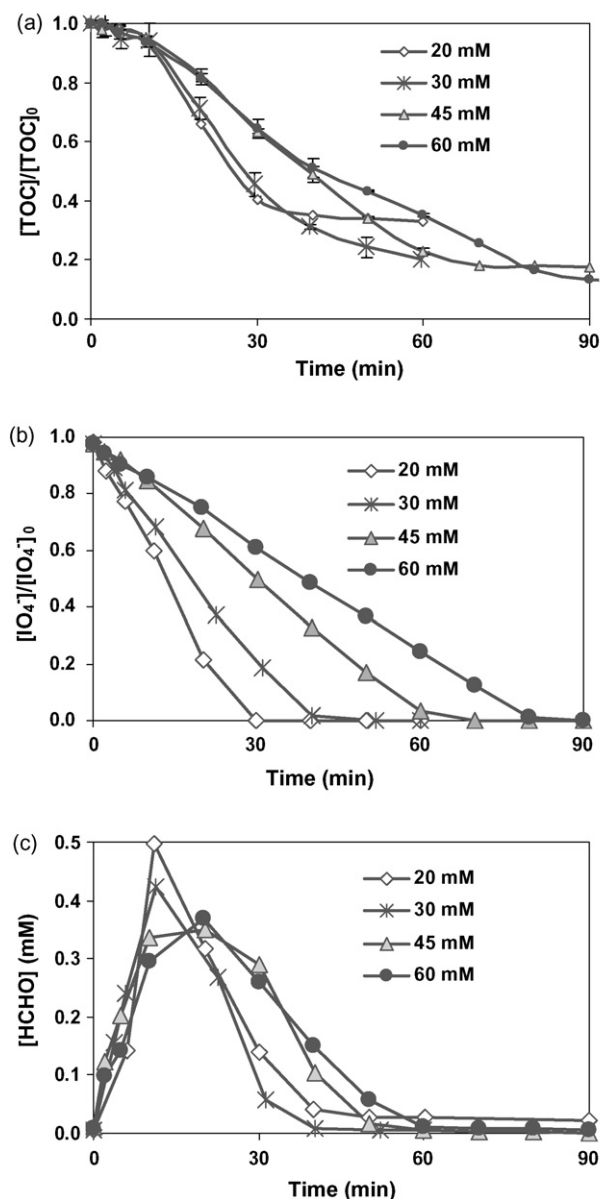


Fig. 2. TOC (a), periodate loss (b), and formaldehyde formation (c) from 1 mM TDG in the presence of light at various periodate concentrations at pH 3.

in all systems at periodate concentrations from 20 to 60 mM. Fig. 2a shows that there appears to be a lag time before mineralization begins. In addition, mineralization ceases when periodate is depleted from the system. The final TOC level decreased as the initial periodate concentration increased as shown in Table 2 and Fig. 2a. Interestingly, the rate of TOC loss appears to be higher at lower periodate concentration. As with degradation products, TOC loss profiles in TDG systems are similar to that for TDP and TX although the extent of TOC loss and time to reach final TOC values varied.

Periodate concentration effects on periodate reaction kinetics were also investigated. Similar to Fig. 1b, periodate loss followed zero-order kinetics for all concentrations of periodate with TDG, TDP, and TX. Dividing slopes in Fig. 2b by $[IO_4^-]_0$ (i.e., $k = \text{slope}/C_0$) verifies periodate loss follows zero-order kinetics. Formaldehyde formation was investigated with changing initial IO_4^- concentrations (see Fig. 2c). The concentration of formaldehyde reaches its highest concentration with lowest initial IO_4^- concentrations. Moreover, the formation of formaldehyde is significantly higher in the TDG systems than the TDP and TX systems (data not shown). In all cases the formaldehyde peak decomposed rapidly coincident with the loss of TOC. Therefore, the oxidation of formaldehyde in the system appears to be responsible for carbon mineralization. Higher concentrations of formaldehyde produced with lower initial $[IO_4^-]$ corresponded to a higher rate of TOC loss. Because IO_4^- loss is dominated by photolysis following zero-order kinetics, the amount of radicals generated from photoactivated periodate is expected to be the same at each initial periodate concentration. Thus, a higher initial concentration of IO_4^- is competing with HCWA and reaction products for radicals (Eq. (3)). This competition appears to slow the TOC mineralization process.

3.3. N_2 purging

$O(^3P)$ has been speculated to be an important species in UV/ IO_4^- systems [10]. It is able to either react directly with target compounds or combine with molecular oxygen to form ozone by Eq. (4). Based on reactions in variable O_2 environments, ozone was reported to be a much less reactive species than $O(^3P)$ with 4-chlorophenol [10]. In order to investigate the effect of oxygen in the UV/ IO_4^- /HCWA systems, a high flow rate of

Table 2
Resulting TOC concentration and % TOC loss after IO_4^- depletion under various conditions

Conditions		TDG		TDP		TX	
pH	IO_4^- (mM)	TOC (mg L ⁻¹)	% Loss	TOC (mg L ⁻¹)	% Loss	TOC (mg L ⁻¹)	% Loss
3	0; no UV	48.0	0	72.0	0	48.0	0
3	15	23.0	52	ND ^a	ND ^a	ND ^a	ND ^a
3	20	15.8	67	47.5	34	34.6	28
3	30	10 ± 1	79 ± 2	38.1 ± 0.2	47.1 ± 0.3	29.8 ± 0.8	38 ± 2
3	45	8.2	83	29.5	59	20.2	58
3	60	6.2	87	23.0	68	13.9	71
7	30	21 ± 1	56 ± 2	48 ± 3	33 ± 4	33.6	30
10	30	19.2	60	46.1	36	22.1	54
3	30, N ₂ purging	7.2	85	31.0	57	25.0	48
3	3 × 20	3.8	92	8.6	88	5.3	89

^a Not determined.

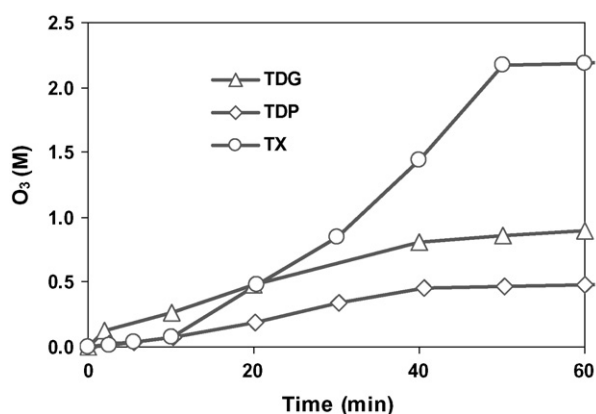


Fig. 3. Accumulated O_3 collected by continuous N_2 purging of the photoactivated periodate system at pH 3 with 1 mM HCWA and $[IO_4^-]_0 = 30$ mM.

nitrogen gas used to purge the systems to provide an oxygen limited environment. The extent of mineralization was improved by reducing O_2 in the system as shown in Table 2. Thus, oxygen limited conditions are favorable in UV/ IO_4^- /HCWAs systems. Reducing O_2 available to react with $O(^3P)$ is expected to increase the $O(^3P)$ available to react with other compounds in the system. This demonstrates that $O(^3P)$ is an important radical in the reactions.

Any O_3 removed from the photochemical reactor during purging was collected and analyzed with time as shown in Fig. 3. Although O_2 was continuously removed, it was generated through Eq. (6) and/or Eq. (9) allowing for O_3 formation. O_3 collected was the highest in the slower reacting TX system. TDP, with the highest initial TOC, had the least amount of O_3 collected. This trend may indicate: (1) OH^\bullet is less reactive with TX compared with TDG and TDP resulting in more IO_4^- regeneration through reaction of OH^\bullet with IO_4^- (Eqs. (3) and (6)) in the TX system; (2) IO_4^\bullet is less reactive with TX compared with TDP and TDG allowing more IO_4^\bullet dimerization reactions to generate O_2 and IO_4^- in the slower reacting system; (3) $O(^3P)$ is less reactive with TOC in the TX system; or (4) a combination of the above.

3.4. Consecutive IO_4^- additions

In order to reduce radical quenching by IO_4^- observed at high IO_4^- concentrations (60 mM), consecutively adding 20 mM IO_4^- at 30 min intervals to a $[IO_4^-]_0 = 20$ mM solution twice (3×20 mM IO_4^-) was investigated to determine TOC reduction compared to $[IO_4^-]_0 = 60$ mM systems. In the first 30 min, 67% of TDG was mineralized as shown in Fig. 4. In the second and third 30 min, an additional 25% of the residual TOC was mineralized. Similar results were observed with TDP and TX systems (Table 2). Thus, three consecutive additions of 20 mM periodate mineralized significantly more HCWAs than one initial 60 mM periodate dose as shown in Table 2. Less TOC loss during the second and third injections suggests that more recalcitrant species and components that quench OH^\bullet such as bicarbonate were produced as the reaction proceeded.

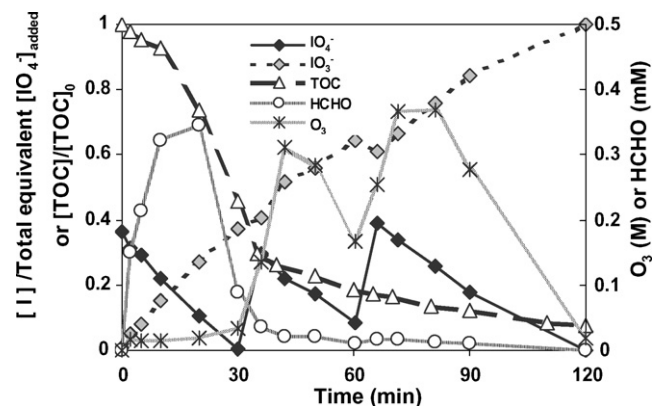


Fig. 4. Loss of TOC associated with TDG in the photoactivated periodate system at pH 3 and $[IO_4^-]_0 = 20$ mM with two additions of 20 mM IO_4^- at 30 and 60 min.

3.5. Effect of pH

Next, the role of pH was explored. At pH 7, TOC loss decreased for all compounds compared to pH 3 (Fig. 5 and Table 2). Fig. 5 shows similar amounts of formaldehyde formation at pH 3 and 7, although at pH 7 it takes longer for formaldehyde to decay. The same speciation of periodate and HCWAs at pH 3 and 7 was assumed to result in similar photolysis reactions. However, O_3 behavior is significantly altered by pH. O_3 decomposes to hydroxyl radical by reaction with OH^- [22]. In addition, mineralization reactions forming bicarbonate, the dominant carbonate species at pH 7, scavenge hydroxyl rad-

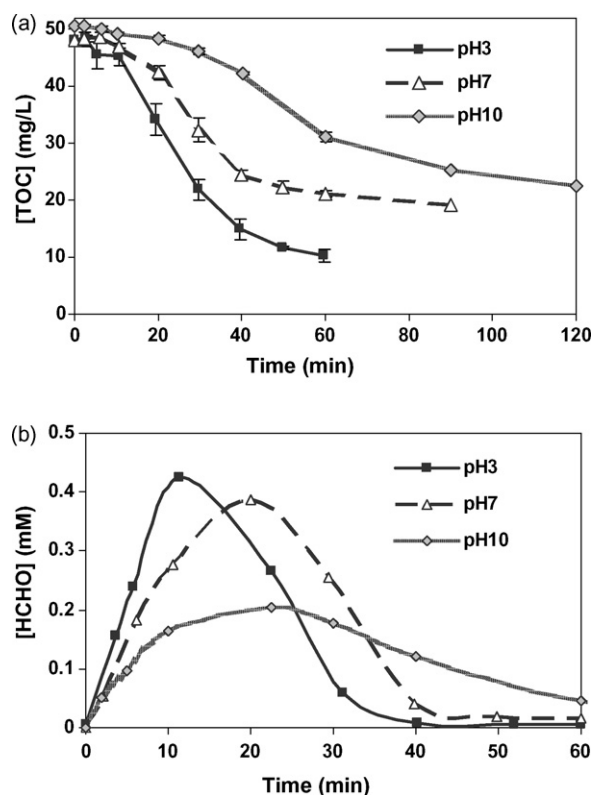


Fig. 5. pH effects on TOC loss (a) and HCHO formation (b) during degradation of TDG in the presence of photoactivated periodate ($[IO_4^-]_0 = 30$ mM).

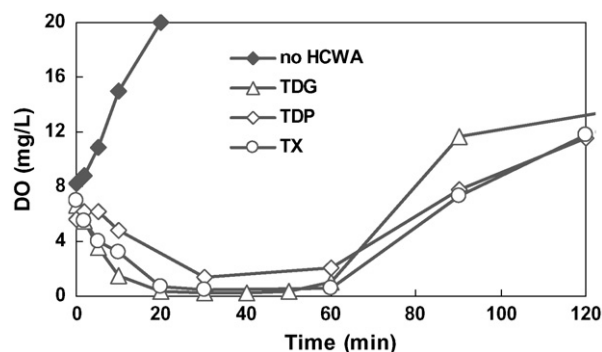


Fig. 6. Dissolved oxygen at $[\text{IO}_4^-]_0 = 30 \text{ mM}$ in the presence and absence of HCWAs at pH 10 during photolysis.

icals and impede the loss of TOC [34]. Therefore, the rates of TOC loss were slower at pH 7 compared to pH 3 (Fig. 5b).

On the other hand, slower degradation of IO_4^- at pH 7, compared to the same conditions at pH 3 (Table 1), suggests that regeneration of IO_4^- is more favorable at pH 7 than at pH 3. Increased OH^\bullet present at pH 7 may react with IO_4^- and IO_3^- to form IO_4^\bullet and IO_3^\bullet , regenerating IO_4^- through IO_4^\bullet and IO_3^\bullet dimerization reactions (Eqs. (5)–(8)).

Different periodate speciation at pH 10 compared to low pH results in a different photolysis mechanism and degree of TOC loss [13]. At pH 10, the dominant species are $\text{H}_3\text{IO}_6^{2-}$ and $\text{H}_4\text{I}_2\text{O}_{10}^{4-}$ with significant differences in light absorption compared to pH 3 and 7 [11]. Our results showed a significant decrease in periodate loss in both the presence and absence of HCWAs with an increase in pH (Table 1). As shown in Fig. 6, DO measurements at pH 10 demonstrated a rapid depletion of O_2 at the beginning of reactions and no measurable O_3 . Unlike in the presence of HCWAs, photolysis of periodate in the absence of HCWAs at pH 10 showed an increase in oxygen at the beginning of the reaction as shown in Fig. 6. This result demonstrates that radicals reacting with HCWAs interact with iodine species and periodate.

Differences in degradation of TOC at different pH values for these HCWAs are in conflict with Lee and Yoon showing that dye decomposition by photoactivated periodate has no pH effect [9]. Among the three pH conditions investigated, mineralization of TDG and TDP was the lowest at pH 10 (Table 2). Either the reactivity of the radicals was low or the quantity of radicals generated was less resulting in the slower reactions of TDG and TDP.

Whereas TDG and TDP mineralization slowed at pH 10 compared with pH 3 and 7, mineralization of TX was more favorable at pH 10 than at pH 3 and 7 (Table 2). Again, primary photolysis of periodate is expected to be similar under all conditions at pH 10. Thus, the increase in mineralization of TX at high pH may be due to different radical reactivity at the different pH values. The radicals generated at pH 10 may be more reactive with TX than radicals that were generated at pH 3 and 7. The pH effect observed with TDG and TDP may be due to changes in the rate of the dark reactions or may be due to changes in radical species. An investigation of photoactivated periodate degradation with a compound that does not have dark reaction with periodate would assist in determining the reason for the pH effect. Nevertheless,

the change in TOC loss with pH for the different HCWAs clearly indicates that degradation is selective and compound specific.

3.6. Efficiency of periodate on TOC loss

The rate of TOC loss of HCWAs is not proportional to the total quantity of periodate added to the systems. Therefore, for optimization purposes it is important to investigate the efficiency of periodate acting on HCWAs in the system. The amount of TOC loss to the total quantity of periodate added (expressed as equivalent $[\text{IO}_4^-]_{\text{added}}$) is defined as the periodate mineralization efficiency (PME, $\text{mg L}^{-1} \text{mM}^{-1}$). As

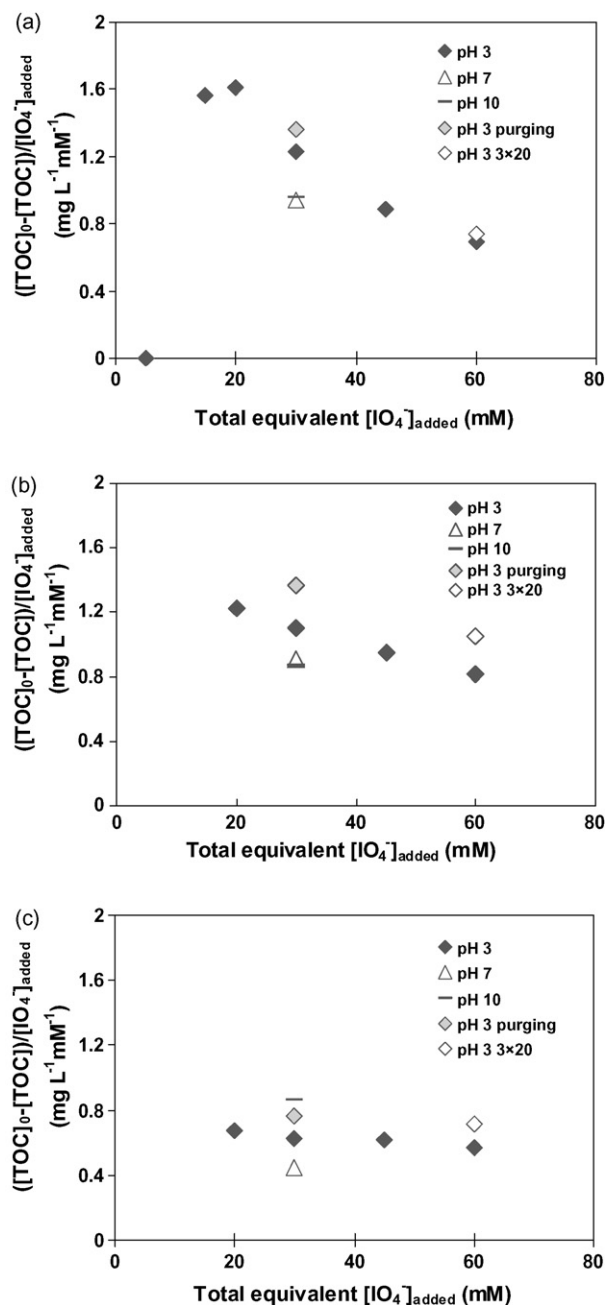


Fig. 7. Periodate mineralization efficiency (PME) under various conditions for TDG (a), TDP (b), TX (c) in UV/ IO_4^- /HCWAs systems.

shown in Table 2, when the quantity of periodate increased, the amount of TOC loss (mg L^{-1}) increased. However, the effectiveness of periodate (i.e., the ability of periodate to impact TOC loss) changed with a total equivalent $[\text{IO}_4^-]_{\text{added}}$ as shown in Fig. 7. This ratio reached a maximum at a total equivalent $[\text{IO}_4^-]_{\text{added}} = 20 \text{ mM}$ at pH 3. As the concentration of periodate increased to 60 mM, PME decreased. Higher concentrations of periodate likely quenched hydroxyl radicals to form periodate radicals that are thought to be less reactive than OH^\bullet (Eq. (3)) [13].

Different PME values at 20 mM IO_4^- added for TDG, TDP, and TX demonstrate that TOC loss and effective use of IO_4^- is affected by the structure of the substrate. The lower PME value of TX demonstrates that the cyclic structure of TX is more difficult to be mineralized than the linear structure of TDG and TDP. Thus IO_4^- is less effectively used with TX compared to TDG and TDP.

Furthermore, PME values are affected by pH. At pH 7, PME values were lower than at pH 3 for all HCWAs. This may due to differences in the speciation of mineralization products (e.g., carbonate and bicarbonate) and ozone reactions at pH 3 and 7. At pH 10, PME values show a similar trend as pH 7 for TDG and TDP. Surprisingly, PME was optimized for TX at pH 10 compared to lower pH or higher periodate concentrations. In addition, opposite to TDG and TDP, formaldehyde production from TX at pH 10 was higher than at low pH (data not shown) resulting in more TOC loss. Because the dark reaction of TX with periodate is slower than TDG and TDP at pH 10 [11], a higher PME value resulted from faster reaction of TX with radicals generated by $\text{H}_3\text{IO}_6^{2-}$ and $\text{H}_4\text{I}_2\text{O}_{10}^{4-}$ at pH 10 compared to low pH.

Although TOC loss of all HCWAs were improved by three consecutive additions of $[\text{IO}_4^-]$ compared to a single addition 60 mM $[\text{IO}_4^-]$, PME values were not significantly improved. The optimal use of periodate determined from PME values was at pH 3 with 20 mM $[\text{IO}_4^-]$ added to TDG; at pH 3 with N_2 purging and 30 mM $[\text{IO}_4^-]$ added to TDP; and at pH 10 with 30 mM $[\text{IO}_4^-]$ added to TX. It is interesting to note that these are all different reaction conditions indicating that the photoactivated periodate system is compound specific and very complex.

4. Conclusions

In this study, the ability of photoactivated periodate to decompose and mineralize HCWAs was demonstrated. Periodate oxidized HCWAs and reaction products were decomposed to form formaldehyde, sulfate and carbon dioxide based on TOC loss. Approximately 90% mineralization of HCWAs was achieved by consecutive additions of 20 mM IO_4^- under polychromatic irradiation at an intensity of $1.76 \mu\text{einstein s}^{-1}$ at pH 3. Both pH and structure of HCWAs play roles in mineralization of HCWAs in the photoactivated periodate system. Furthermore, investigating the PME of different compound is critical for system optimization.

Demonstration of a scaled up photoactivated periodate system on site and detailed investigation of the human health risks associated with handling and treating the material are important

to complete prior to application. Furthermore, the system needs to be further optimized for both energy and cost before application. To our knowledge no other peer-reviewed information is available on TDG, TDP, and TX degradation by other AOPs. Thus, experiments comparing photoactivated periodate to other AOPs are necessary.

Acknowledgements

This material is based upon work supported by the National Science Foundation under Grant No. 0093783. We thank Kari Green-Church at the Mass Spectrometry and Proteomics Facility of the Campus Chemical Instrumentation Center at OSU in assisting in sample analysis.

References

- [1] National Academy Press Recommendations for the Disposal of Chemical Agents and Munitions, Washington, DC, 1994.
- [2] National Academy Press Review and Evaluation of Alternative Chemical Disposal Technologies, Washington, DC, 1996.
- [3] L.R. Ember, Chem. Eng. News 83 (2005) 36.
- [4] O.E. Legrini, A.M. Braun, Chem. Rev. 93 (1993) 671.
- [5] E. Neyens, J. Baeyens, J. Hazard. Mater. 98 (2003) 33.
- [6] P.R. Gogate, A.B. Pandit, Adv. Environ. Res. 8 (2004) 501.
- [7] L.K. Weavers, I. Hua, M.R. Hoffmann, Water Environ. Res. 69 (1997) 1112.
- [8] Y. Wang, C.-S. Hong, Water Res. 33 (1999) 2031.
- [9] C. Lee, J. Yoon, J. Photochem. Photobiol. A: Chem. 165 (2004) 35.
- [10] L.-H. Chia, X. Tang, L.K. Weavers, Environ. Sci. Technol. 38 (2004) 6875.
- [11] X. Tang, L.K. Weavers, J. Photochem. Photobiol. A: Chem. 187 (2007) 311.
- [12] U.K. Klaning, K. Sehested, J. Chem. Soc., Faraday Trans. 74 (1978) 2818.
- [13] U.K. Klaning, K. Sehested, T. Wolff, J. Chem. Soc., Faraday Trans. 77 (1981) 1707.
- [14] I. Wagner, H. Strehlow, Ber. Bunsenges. Phys. Chem. 86 (1982) 297.
- [15] M.S. Subhani, R. Latif, Pak. J. Sci. Ind. Res. 35 (1992) 484.
- [16] G.J. Buist, W.C.P. Hipperson, J.D. Lewis, J. Chem. Soc., Inorg. Phys. Theor. (1969) 307.
- [17] G.J. Buist, The Oxidation of Organic Compounds by Non-metallic Anions. Comprehensive Chemical Kinetics, Elsevier, Amsterdam, The Netherlands, 1972.
- [18] G. Dryhurst, Periodate Oxidation of Diol and Other Functional Groups, Pergamon Press, Oxford, 1970.
- [19] F. Barat, L. Gilles, B. Hickel, B. Lesigne, Chem. Commun. (1971) 847.
- [20] J. Hoigne, H. Bader, W.R. Haag, J. Staehelin, Water Res. 19 (1985) 993.
- [21] D.F. Evans, M.W. Upton, J. Chem. Soc., Dalton Trans. (1985) 1141.
- [22] P. Westerhoff, R. Song, G. Amy, R. Minear, Ozone Sci. Eng. 19 (1997) 55.
- [23] C.G. Hatchard, C.A. Parker, Proc. Roy. Soc. A 235 (1956) 518.
- [24] G.F. Rabek, Experimental Methods in Photochemistry and Photophysics, Part 2, Wiley, New York, 1982.
- [25] S. Honda, K. Suzuki, K. Kakehi, Anal. Biochem. 177 (1989) 62.
- [26] C.E. Kientz, J. Chromatogr. A 814 (1998) 1.
- [27] G. Avigad, Anal. Biochem. 134 (1983) 499.
- [28] H.B. Hopps, Aldrichim. Acta 33 (2000) 28.
- [29] H. Bader, J. Hoigne, Water Res. 15 (1981) 449.
- [30] A.L. Lazrus, G.L. Kok, S.N. Gitlin, J.A. Lind, Anal. Chem. 57 (1985) 917.
- [31] G.L. Kok, T.K. Gitlin, A.L. Lazrus, Anal. Chem. 58 (1986) 1192.
- [32] X. Tang, L.K. Weavers, Applying photoactivated periodate as a technology to decompose hydrolysates of chemical warfare agents (HCWAs), Master Thesis at Ohio State University, 2005.
- [33] P.L. Miller, Y.P. Chin, J. Agric. Food Chem. 50 (2002) 6758.
- [34] J.L. Sotelo, F.J. Beltran, F.J. Benitez, J. Beltran, Ind. Eng. Chem. Res. 26 (1987) 39.